Heliyon 10 (2024) e23687

Contents lists available at ScienceDirect

Heliyon

journal homepage: www.cell.com/heliyon

An immune-related prognostic gene ULBP2 is correlated with immunosuppressive tumor microenvironment and immunotherapy in breast cancer

Rui Feng [a,b,1], Jiali Xu [a,b,1], Jing Huang [c], Jiazhou Liu [a,b], Xiaoyu Wang [a,b], Jing Wang [a,b], Chong Zhang [a,d], Hongzhong Li [a], Yuxian Wei [b,**], Guosheng Ren [a,b,*]

[a] *Chongqing Key Laboratory of Molecular Oncology and Epigenetics, The First Affiliated Hospital of Chongqing Medical University, Chongqing, 400016, China*
[b] *Department of Breast and Thyroid Surgery, The First Affiliated Hospital of Chongqing Medical University, Chongqing, 400016, China*
[c] *Department of Radiology, The First Affiliated Hospital of Chongqing Medical University, Chongqing, 400016, China*
[d] *Department of Ultrasound, The First Affiliated Hospital of Chongqing Medical University, Chongqing, 400016, China*

ARTICLE INFO

Keywords:
ULBP2
Breast cancer
Immune genes
Prognostic model
Tumor microenvironment status
Immunotherapy effect prediction

ABSTRACT

Breast cancer (BC) is one of the major dangerous tumors threatening women's lives. We here aimed to sort out prognostic immune-related genes by univariate Cox regression analysis and build a model of immune-related genes for forecasting the prognosis of BC patients. We identified UL16 binding protein 2 (ULBP2) as a valuable gene for study in the model using related databases and algorithms analysis. We found the stromal and immune cells scores were higher in ULBP2 high expression group and ULBP2 was related to kinds of immune cells, most importantly had negative correlation with $CD8^+$ T cell. Notably, ULBP2 was positively correlated with tumor mutational burden (TMB) and had relationship with many immune checkpoints. Correlation analysis revealed that ULBP2 expression was closely linked to the clinicopathological characters and negatively related to BC patient survival. Gene Ontology (GO) and Kyoto Encyclopedia of Genes and Genomes (KEGG) pathway enrichment analysis showed the functional enrichment of differential genes related to ULBP2. Gene Set Enrichment Analysis (GSEA) indicated pathway enrichment in ULBP2 high and low expression groups. In short, this study comprehensively investigated the potential function of ULBP2 in BC, which might make ULBP2 to be an important therapeutic target for BC.

1. Introduction

Among women, the mortality and morbidity of breast cancer (BC) have occupied the first place among malignant tumors for a long time at a global scale, which is becoming an important factor affecting women's health [1,2]. Although treatments of BC have achieved stunning breakthrough. However, about 30 % of early stage BC patients have multidrug resistance and relapse, and lack effectively

* Corresponding author. Chongqing Key Laboratory of Molecular Oncology and Epigenetics, The First Affiliated Hospital of Chongqing Medical University, Chongqing, 400016, China.
** Corresponding author.
E-mail addresses: saltish0301@163.com (Y. Wei), rengs726@126.com (G. Ren).
[1] These authors have contributed equally to this work and share first authorship.

https://doi.org/10.1016/j.heliyon.2023.e23687
Received 8 April 2023; Received in revised form 29 November 2023; Accepted 9 December 2023
Available online 14 December 2023

targeted treatment [3]. Therefore, a comprehensive bioinformatics investigation of the BC genes is urgently needed to identify more potential genes as targets for therapy and to predict the prognosis of the disease.

The immune system is crucial for the development of cancers. The aim of modulation of immune system in cancer therapy is boosting $CD8^+$ T lymphocytes, natural killer (NK) cells or other immune cells, as well as suppression of immunosuppressive responses by macrophages and regulatory T cells (Tregs) [4]. Now, immunotherapy of the cancer therapies can cure cancer, prevent recurrence and metastasis, and ultimately eradicate cancer by restoring and enhancing the immune monitoring of cancer patients and the function of poisoning cancer cells. This therapy is a promising treatment mode for BC, and the immune system can intervene the effect of immunotherapy of BC patients [4–7]. Moreover, immune-related genes (IRGs) in tumor cells, which are either up-regulated or down-regulated, may be related to patient outcomes. Thus, it is requisite to engage in bioinformatics research to comprehensively explore IRG expression profile in BC.

Then we built an independent risk score model to predict BC patients' prognosis and found a very valuable gene, UL16 binding protein 2 (ULBP2). Compared to other genes in the model, there is relatively little research on ULBP2 in BC, and we find it can affects immune response in BC patients by binding to the receptor of NK cells and subsets of T cells [8]. Lately, it is reported that ULBP2 has an inhibitory effect on the development of BC after being knocked down [9]. Thus we performed significant amount of explore to reveal that ULBP2 may be a crucial gene marker of BC with powerful functions.

2. Materials and methods

2.1. Data source

RNA-seq data of BC samples and their clinical data were downloaded from the TCGA database (http://portal.gdc.cancer.gov). Data sets of IRGs and transcription factor (TF) were acquired from the Immport (https://www.immport.org) and Cistrome database (https://cistrome.org) respectively [10].

2.2. Screening of differentially expressed transcriptome genes, IRGs and TFs

The ggplot2 and Pheatmap packages were applied to obtain differentially expressed transcriptome genes (DEGs), IRGs and TFs in tumor tissues and normal tissues. $p < 0.05$ and $|\log2\ \text{FC (fold-change)}| > 1$ were screening criteria.

2.3. Construction of a prognostic-associated IRGs model

We conducted univariate Cox regression analysis for selecting the prognostic IRGs, $p < 0.001$ was the filtration criteria. The regulatory network of interactions of TFs and prognosis-associated IRGs was displayed using Cytoscape software [11]. Through the filter condition ($p < 0.001$), only five prognosis-associated IRGs were selected for constructing a prognostic model and the risk score of BC patients was computed by $\sum(\text{ExpmRNA1} - \text{nxcoefmRNA1} - \text{n})$. In this formula, "Exp" and "coef" respectively represent gene expression and gene correlation coefficient, "mRNA" and "n" respectively represent specific genes and the number of genes. We plotted the survival curves of the high-risk and low-risk groups by survival and survminer packages of R software, and the ROC curve was used to assess the model's accuracy. We also performed a prognosis analysis with single and multi-factors.

2.4. The ESTIMATE and CIBERSORT algorithm

The ESTIMATE package computed stromal, immune and estimate scores. CIBERSORT algorithm was uesd to expose the content of 22 kinds of immune cells ($p < 0.05$). Spearman correlation analysis was conducted to analyze the relationship between ULBP2 and each immune cell ($p < 0.05$).

2.5. Correlation analysis between ULBP2 and immune checkpoints and tumor mutational burden (TMB)

We explored the association between ULBP2 and immune checkpoint with pearson correlation analysis. Similarly, spearman correlation analysis was utilized to show association of ULBP2 and TMB.

2.6. The nomogram

We first revealed the correlation between ULBP2 and the clinical features of BC patients with limma, ggpubr and ComplexHeatmap package. We delineated the nomogram to predict the survival probability of BC patients by integrating clinical characters of BC patients and ULBP2 expression. Calibration curve estimated accuracy of the nomogram.

2.7. Analysis of genes related to ULBP2

Through pearson correlation analysis, we found genes with significant correlation with ULBP2 ($p < 0.001$). We used clusterProfiler package to conduct Gene Ontology (GO) and Kyoto Encyclopedia of Genes and Genomes (KEGG) pathway enrichment analysis of ULBP2-related genes (pvalueFilter = 0.05, qvalueFilter = 0.05). We also performed Gene Set Enrichment Analysis (GSEA) in different

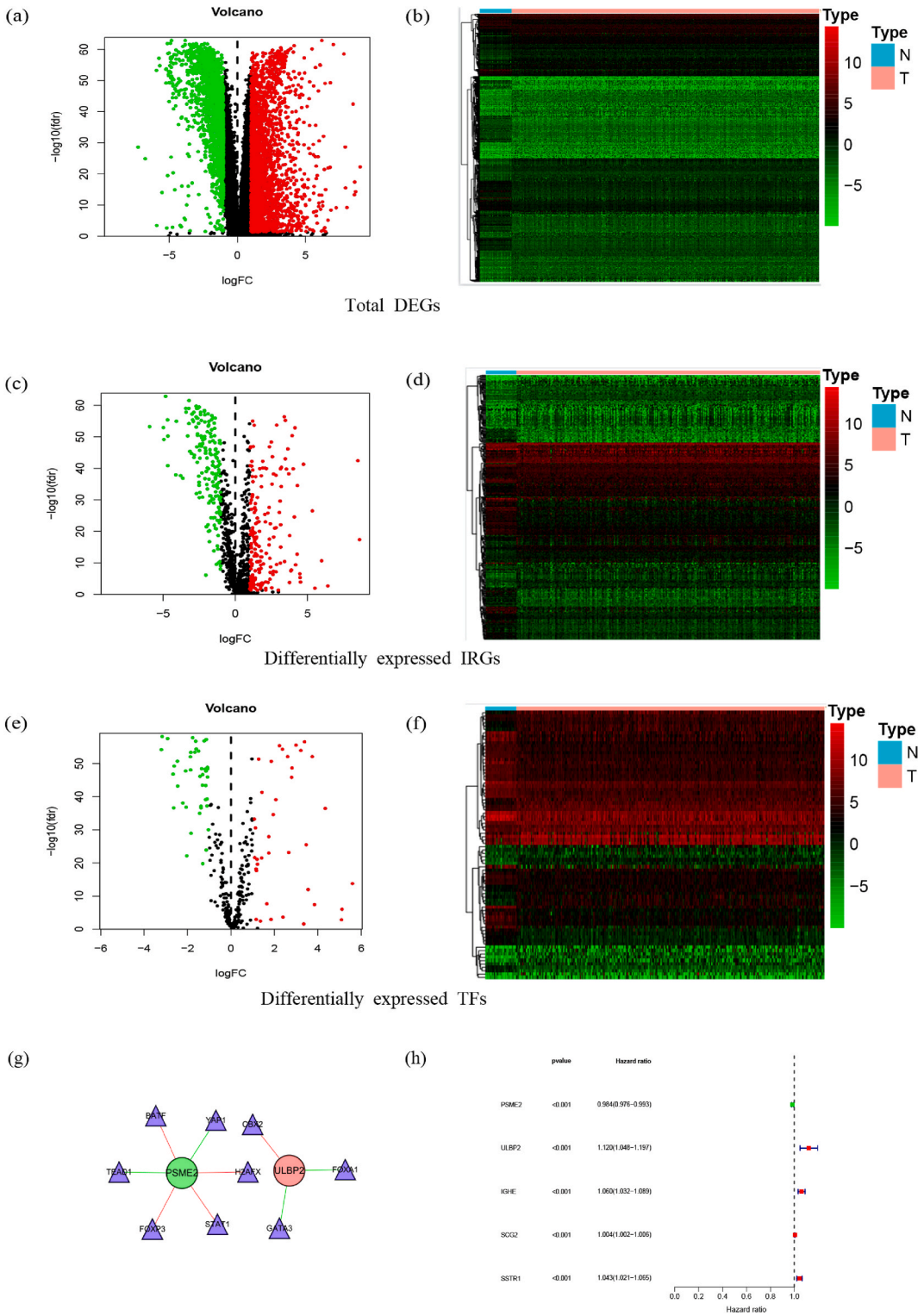

Fig. 1. Screening of differential genes of BC patients. **(a, b)** the volcano map and heatmap showed total differential genes, the color bar means logFC. **(c, d)** the volcano map and heatmap showed differential immune-related genes, the color bar means logFC. **(e, f)** the volcano map and heatmap showed differential TFs. DEGs were detected by Wilcoxon rank sum test (|log2FC| > 1 & fdr <0.05), the color bar means logFC. **(g)** In the interaction network, the red and green ellipsoidal nodes represent IRGs with high- and low-hazard ratios respectively. The red and green edges indicate positive- and negative-regulatory relationships respectively. **(h)** Univariate Cox analysis of IRGs and prognostic information of BC patients. Five prognosis-associated IRGs were screened out by drawing the forest map ($p < 0.001$).

expression groups of ULBP2.

3. Results

3.1. Differentially expressed IRGs and TFs were screened out

Our study contained 1109 BCE samples and 113 normal samples. Then, we screened out 4575 DEGs in BC, among which, 2698 and 1877 genes were up-regulated and down-regulated, respectively (Fig. 1a and b). In addition, we obtained IRGs from the Immport database and intersected them with the 4575 DEGs mentioned above to obtain 370 differentially expressed IRGs, containing 194 up-regulated IRGs and 176 down-regulated IRGs in BC (Fig. 1c and d).

Similarly, after that TFs were obtained from the Cistrome database, we intersected them with 4575 DEGs and got 80 differentially expressed TFs, containing 38 up-regulated TFs and 42 down-regulated TFs in BC (Fig. 1e and f). Through the filter condition ($p < 0.001$), five IRGs related to prognosis were obtained using univariate Cox regression analysis between differentially expressed IRGs and the survival data, among which, the risk genes were ULBP2, IGHE, SCG2 and SSTR1, and the protective gene was PSME2. The association between differentially expressed TFs and five prognostic IRGs was investigated and their interaction regulatory network was shown in Fig. 1g.

One protection gene and four risk genes were employed to generate the forest map (Fig. 1h). Generally, Hazard ratio (HR) > 1 and $0 < HR < 1$ suggest that genes are prognostic risk factors and prognostic protection factors, respectively.

3.2. The prognostic model revealed BC patients with the increase of risk score had worse prognosis

The prognostic model was constructed by using the five screened IRGs related to prognosis (Table 1). We computed the risk scores of BC patients. We divided the patients into high risk and low risk groups by the median of risk value. Then, we drew the KM survival curve to demonstrate the relationship between the high or low risk group and the survival time (Fig. 2a). As the survival time increased, the survival rate of high and low risk groups gradually decreased. However, the survival rate of high risk group was lower at the same survival time. We also drew the ROC curve and the area under the curve was AUC = 0.687 (Fig. 2b), indicating that the constructed model had significant accuracy in predicting prognosis.

We ranked the risk score of BC patients from low to high (Fig. 2c) and took median value as the dividing point. The scatter plot was used to display the survival status and time of two risk groups (Fig. 2d). It indicated that dead patients gradually increased and patients' survival time gradually decreased with the increase of risk score. Therefore, the results showed that the risk score was an adverse factor in predicting prognosis. Our results also further revealed the differential expression of the five prognosis-associated IRGs in the two risk groups by drawing the heatmap (Fig. 2e).

Univariate independent prognostic analysis of BC patients was performed with gender, age, grade, stage, TNM stage and risk score (Fig. 2f). We found that risk score, age, stage and TNM stage were independent factors for predicting patient prognosis. According to $HR > 1$, we could know they were the prognostic risk factors. We also conducted multivariate independent prognostic analysis with all indicators. It demonstrated that the risk score, age, M stage and N stage of BC patients could independently predict patient prognosis ($HR > 1$) (Fig. 2g).

3.3. ULBP2 indicated the status of tumor microenvironment and was related to the effect of immunotherapy of BC patients

Through the follow correlative analysis, we found that ULBP2 played a critical role for BC patients. In our research, we performed TIDE algorithm analysis and found high CTL levels indicated better prognosis of BC patients with low ULBP2 expression levels in tumor tissues (Fig. 3a). But when the expression levels of ULBP2 was high, high CTL levels indicated the poor prognosis. These data indicated that the high expressions of ULBP2 was closely related to T cell dysfunction, thus affecting the prognosis of BC patients. To clarify the effect of ULBP2 as an immune gene in the tumor microenvironment of BC, we estimated stromal cells score and immune cells score and detected the content of 22 types of immune cells of BC tumor microenvironment in ULBP2 high and low expression groups through the ESTIMATE and the CIBERSORT algorithm. The violin plot depicted high ULBP2 expression caused raised stromal and immune cells content in BC patients (Fig. 3b). Besides, Fig. 3c showed that the fractions of the naïve B cells, $CD8^+$ T cells, resting memory $CD4^+$ T cells, monocytes, resting dendritic cells and resting mast cells in ULBP2 high expression group was comparatively less than that in ULBP2 low expression group, and activated memory $CD4^+$ T cells, resting NK cells, M0 macrophages, activated dendritic cells and

Table 1
Prognosis-associated IRGs in the model.

id	coef	HR	HR.95L	HR.95H	*p*value
PSME2	−0.015576898	0.984543795	0.975950248	0.99321301	0.000496781
ULBP2	0.120383218	1.127929011	1.053869404	1.207193082	0.000512447
IGHE	0.065430253	1.067618272	1.039917919	1.096056481	1.07E-06
SCG2	0.004153042	1.004161678	1.002013446	1.006314515	0.000144245
SSTR1	0.045535248	1.046587894	1.024223307	1.069440827	3.60E-05

HR, hazard ratio.

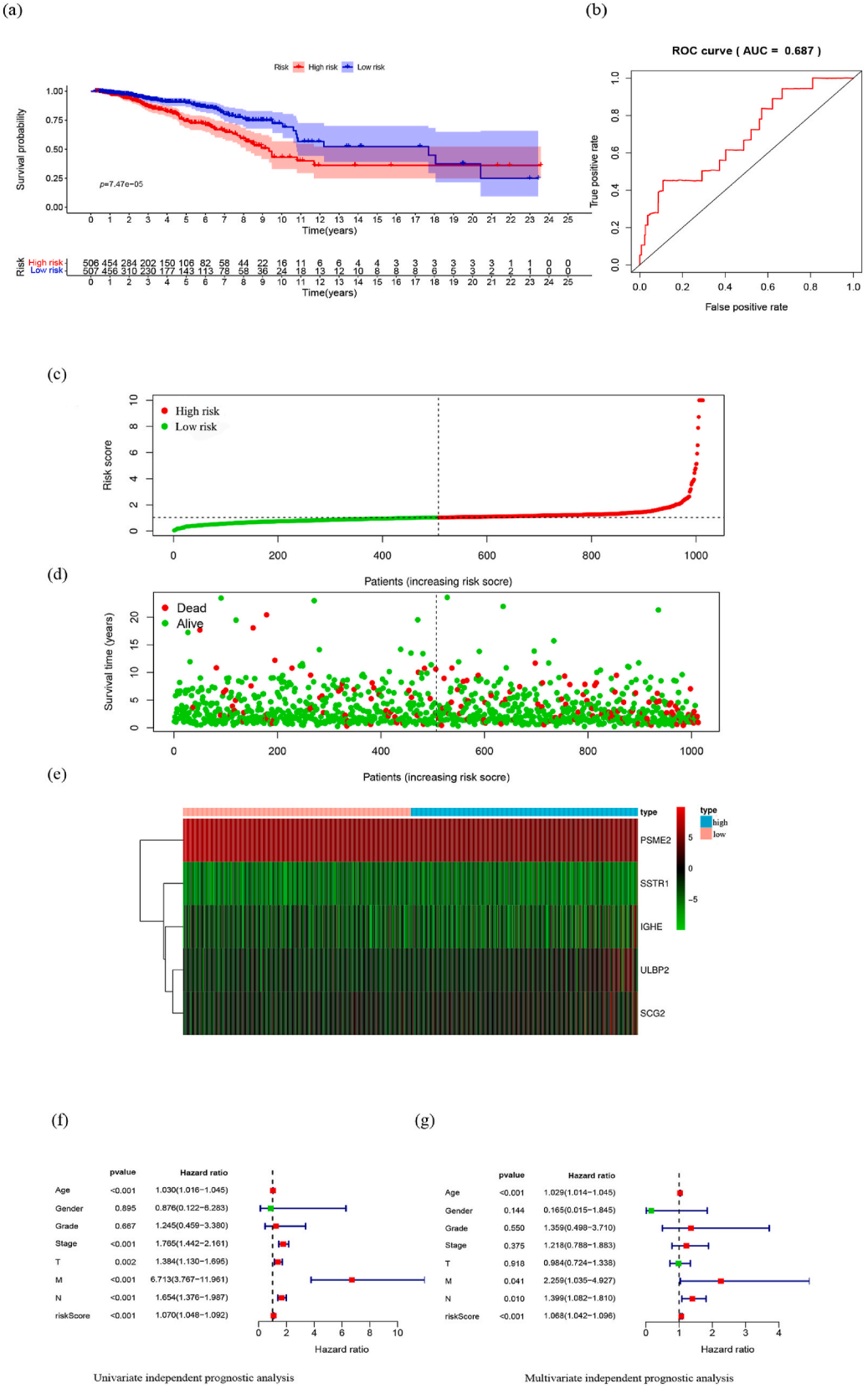

(caption on next page)

Fig. 2. The risk score of the model is an important indicator of the survival of BC patients. **(a)** Kaplan–Meier curve of OS of BC patients. The differences between the two curves were evaluated by the two-side log-rank test. **(b)** The ROC curve analysis was used to evaluate the accuracy of the model. **(c)** Risk score distribution of the BC patients. **(d)** Presenting of survival status of BC patients. **(e)** Expression profile of five IRGs, the color bar means logFC. **(f)** Prognostic factors including age, stage, TNM stage and risk score were detected by univariate independent prognostic analysis ($p < 0.05$). **(g)** Prognostic factors including age, NM stage and risk score were detected by multivariate independent prognostic analysis ($p < 0.05$).

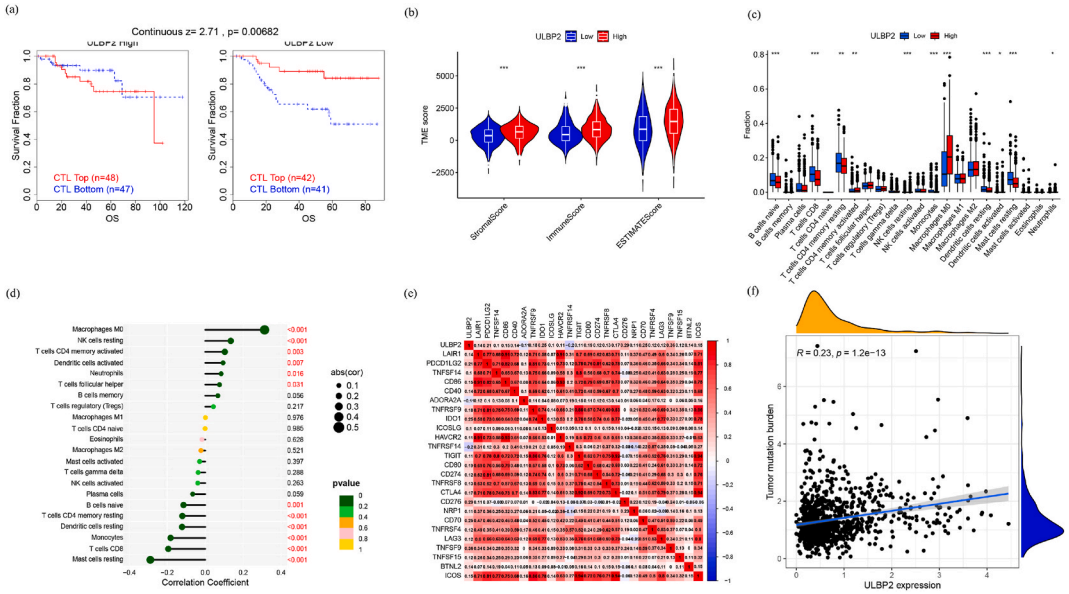

Fig. 3. ULBP2 was related to TME score, immune cell infiltration, checkpoints and TMB. **(a)** The association between the CTL level and OS of BC patients with different ULBP2 levels. **(b)** stromal cell score and immune cell score in ULBP2 high and low expression group. **(c)** The content of different kinds of immune cells in the high and low expression group of ULBP2. Spearman correlation analysis was the statistical methods. **(d)** the relationship of various kinds of immune cells and ULBP2. **(e)** ULBP2 had significant correlation with different checkpoint. Pearson analysis evaluates the significance of correlation. **(f)** ULBP2 was positively related to TMB. P value are based on spearman analysis.

neutrophils were moderately greater in ULBP2 high expression group. Finally, we applied this Lollipop figure to express the relationship between ULBP2 and immune cells (Fig. 3d). We could see that the first six cells were positively correlated with ULBP2 and the last six cells were negatively correlated with ULBP2. From the above, it could be seen that, ULBP2 was correlated with immunosuppressive tumor microenvironment.

Increasingly evidence illustrates that immunotherapy, as one of the cancer treatment methods, has developed rapidly and achieved more and more considerable effect. Here, pearson analysis revealed the association among ULBP2 and immune checkpoint-related genes (Fig. 3e). There were 26 immune checkpoint-related genes that had significant interrelatedness with ULBP2 ($p < 0.001$). Moreover, detection of tumor mutation burden of malignant tumors can forecast the effect of patients on immunotherapy. Presently, it has become a new biomarker with good prospects to predict the effect of cancer immunotherapy in clinical practice. Spearman correlation analysis indicated the significant positive relationship between ULBP2 and TMB (Fig. 3f). In general, ULBP2 had potential predictability in the immunotherapy effect of BC patients.

3.4. ULBP2 was negatively correlated with the prognosis and had significant intrinsic links with the clinicopathological characteristics of BC patients

Our results further revealed that ULBP2 was related to poor prognosis of BC patients. Firstly, ULBP2 expression were sorted out from the data of the above BC and normal samples. It could be clearly seen that expression of ULBP2 was obviously distinct between BC patients and normal people, even the paired normal tissues by limma package, ggplot2 package and ggpubr package in R software (Fig. 4a and b). We could also obtain a similar result that ULBP2 expressed higher in breast tumor tissues by the HPA dataset (https://www.proteinatlas.org/) (Fig. 4c and d). Then we investigated the correlativity between ULBP2 expression and prognosis. This study performed Kaplan-Meier survival analysis to study Overall Survival ($P = 0.00049$), Distant Metastasis-Free Survival ($P = 0.0025$), Period Progression Survival ($P = 0.0038$), Recurrence Free Survival ($P = 0.0025$), Progression-Free-Survival ($p = 0.050$) of BC patients and showed that high expression of ULBP2 was associated with poor prognosis (Fig. 4e–i).

Given the repercussions of ULBP2 expression on BC patients survival, we futher explored the relationship between ULBP2 and the clinical features. In Fig. 4j and k, the expression of ULBP2 was higher in the groups of younger than 65 years old and female. In respect of the T-staging figure, we could also discover that ULBP2 expressed higher in the high level stage (Fig. 4l). After that, based on ULBP2 median expression, we allocated BC patients into ULBP2 high and low expression groups. The heatmap elucidated that patient's gender

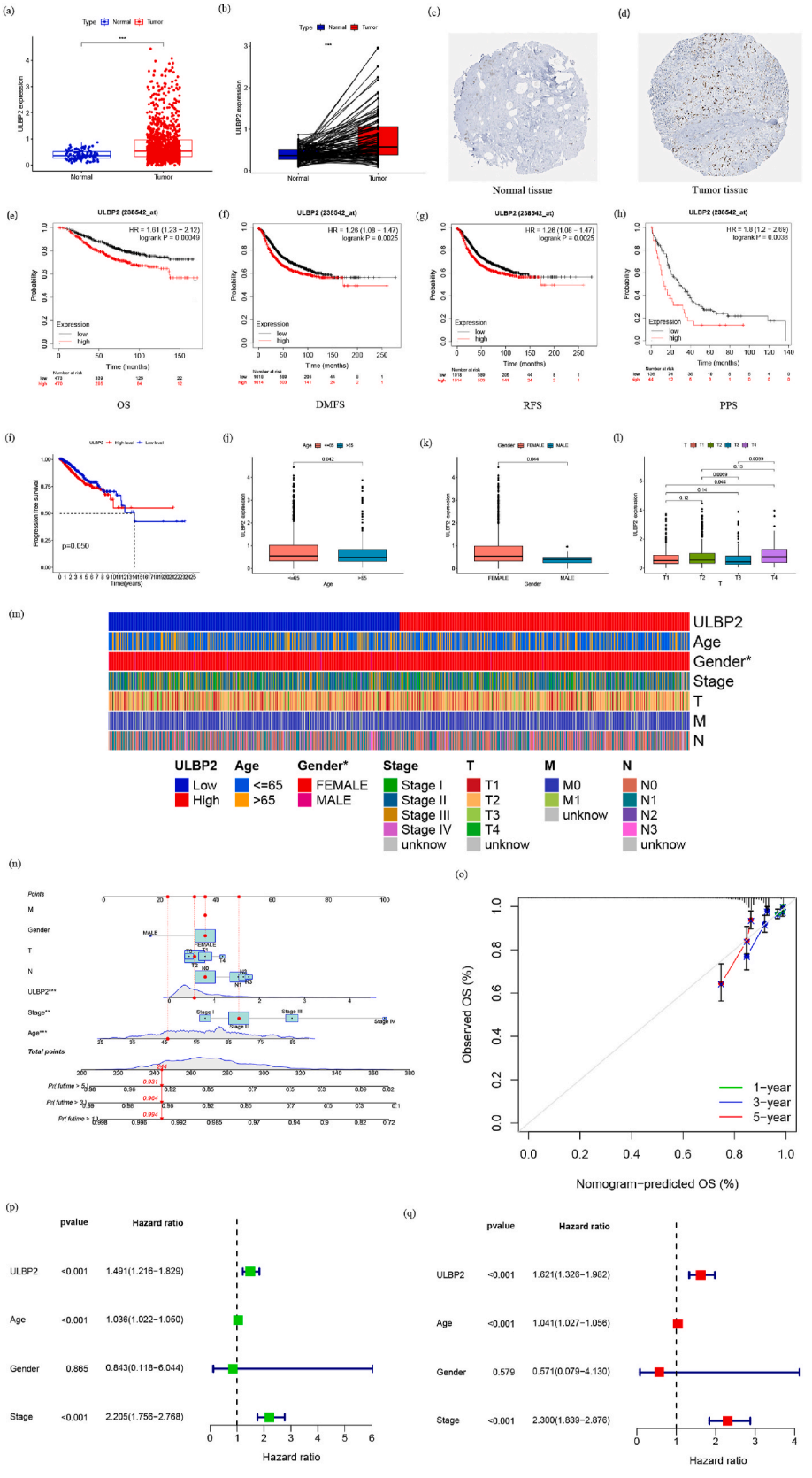

(caption on next page)

Fig. 4. The expression of ULBP2 and association with survival of BC patients and clinicopathological characterastics. **(a)** Differential expression of ULBP2 in BC and normal tissues. Statistical method was Wilcoxon-Mann-Whitney test. **(b)** ULBP2 expression levels in the paired BC tissues were evaluated. P-value was detected by the Wilcoxon Test. **(c–d)** The IHC of ULBP2 expression in BC and normal tissue in the HPA dataset. **(e–i)** The relationship of ULBP2 expression and OS, DMFS, RFS, PPS, PFS of BC patients by KM survival analysis. **(j–l)** The correlation of ULBP2 expression with age, gender and T-stage of BC patients by Wilcoxon rank sum test. **(m)** Enrichment of clinical features in different expression groups of ULBP2. **(n)** Nomogram model was used to predict the probability of 1-, 3-, and 5-year OS of BC patients. Points are assigned for clinical features. The total points axis shows the sum of all these points. The total points on the bottom scales correspond to the forecast of 1-, 3-, and 5-year survival probability. **(o)** Calibration curve of the nomogram at 1-, 3-, and 5-year. The X-axis is nomogram-predicted OS. The Y-axis is observed OS. **(p–q)** independent prognostic analysis of BC patients with ULBP2, age, gender, stage.

was different in the two groups ($p < 0.05$) (Fig. 4m). Furthermore, a prognostic nomogram was manufactured about BC patients to forecast the survival probability by considering M, gender, T, N, the expression of ULBP2, stage, and age (Fig. 4n). Calibration of the nomogram was also conducted (Fig. 4o). This figure showed that the calibration curve (1-year, 3-year, 5-year) was close to the diagonal line, which represented that the nomograph had an acceptable accuracy. In order to discern whether ULBP2 could become an independent prognostic factor after comparing with other clinical characteristics. Our study completed univariate and multivariate independent prognostic analysis with ULBP2, age, gender and stage (Fig. 4p and q). We found that ULBP2 expression could independently predict patient prognosis (The P value of both analysis <0.001).

3.5. The transcriptome of BC patients was impacted by ULBP2 extensively

After observing the considerable influence of ULBP2 on the prognosis and clinical features, we were interested in exploring the effect of ULBP2 expression on other gene expression in patients' transcriptome. We picked out the genes that had strong co-expression relationship with ULBP2 in the transcriptome data (the filter criteria set were $|cor| > 0.3$ and the $P < 0.001$, respectively), and the results showed the top 6 genes among the 56 genes merely (Fig. 5a). Next, we utilized the 5 genes with the smallest correlation coefficient and the 5 genes with the largest correlation coefficient to draw a circle graph (Fig. 5b). Moreover, we drawn the heatmap for evincing the top 50 genes with the significant up-regulated and down-regulated respectively in the ULBP2 high expression group (Fig. 5c). GO analysis was used to show the functions enriched by DEGs (Fig. 5d). According to the p value of enrichment significance, we selected the top 6 from Biological Process, Molecular Function and Cellular Component to draw the circle graph of GO (Fig. 5e). The barplot principally manifested the enrichment pathway of Neuroactive ligand−receptor interaction, Cytokine−cytokine receptor interaction and cAMP signaling pathway by KEGG pathway analysis (Fig. 5f). Moreover, we performed GSEA to investigate the gene sets enriched in ULBP2 subgroups. The genes in the low expression group of ULBP2 were markedly enriched in metabolic pathways, while those genes in the high expression group were chiefly enriched in focal adhesion, leukocyte transendothelial migration and endocytosis. In general, these results intimated that ULBP2 affected the transcriptome of BC patients tremendously.

4. Discussion

As the most common malignancy, BC intensively threatens women's lives. In recent years, there have been major advance in the study and treatment of BC, but there is still no effective therapeutic target. A growing number of research have suggested that cancer immunotherapy, especially the treatment of immune checkpoint inhibitors, has played a key role in some cancers treatments and had sustained therapeutic effects and affected the prognosis of patients [12]. Previous study showed that IRGs can affect the activation and spread of tumor immune cells to a great extent, and may further affect the immunotherapy and prognosis of patients [13–17]. In addition, each cancer has specific IRGs, it is necessary to study the IRGs of patients with BC for exploring effective immunotherapy strategies and predicting prognosis.

Our study identified and built five IRGs risk score model by a large amount of bioinformatics analysis, which include PSME2, ULBP2, IGHE, SCG2 and SSTR1. The risk score was an independent prognostic factor of BC patients. More importantly, among the above five IRGs, we found that ULBP2 was closely correlated with patients' prognosis and had numerous significant functions in BC.

ULBP2 is a ligand of natural killer group 2 member D and mainly expresses in intestinal mucosal epithelial cells and epithelial tumor cells under stress condition. Likewise, a study using immunohistochemistry technique had shown that ULBP2 had heterogeneous expression in different metastatic tumors, and soluble ULBP2 might mean the prognosis of patient was poor [18]. In another research, soluble ULBP2 was important in the immunoregulation of pancreatic cancer, the *vitro* study showed that soluble ULBP2 in pancreatic cancer cells inhibited the expression of natural killer group 2 member D and reduced the cytotoxicity of NK cells, which might influence the outcome [19]. In addition, ULBP2 also analogously plays an anti-tumor role in BC. As we know, TME affects the occurrence and development of cancer, which contains tumor cells, stromal cells and immune cells [20,21]. Likewise, concerning the significance of immune cell infiltration in tumors [22–24], ESTIMATE and CIBERSORT assessed the content of immune cells and stromal cells and the abundance ratio of 22 kinds of immune cells. In ULBP2 low expression group, the naïve B cells, $CD8^+$ T cells, resting memory $CD4^+$ T cells, monocytes, resting dendritic cells and resting mast cells had higher proportions. While in ULBP2 high expression group, the content of activated memory $CD4^+$ T cells, resting NK cells, M0 macrophages, activated dendritic cells and neutrophils was higher, meaning that the expression of ULBP2 inhibits the differentiation and activation of some immune cells in BC. With further analysis, we found that ULBP2 was correlated with some immune checkpoints and positively related to TMB. As we all know, great progress has been made in the development of immune checkpoint inhibitors for treating BC, but they still face enormous challenges [25]. TMB has been well known to foresee the effect to immune checkpoint inhibitors [26]. Therefore, ULBP2 might become

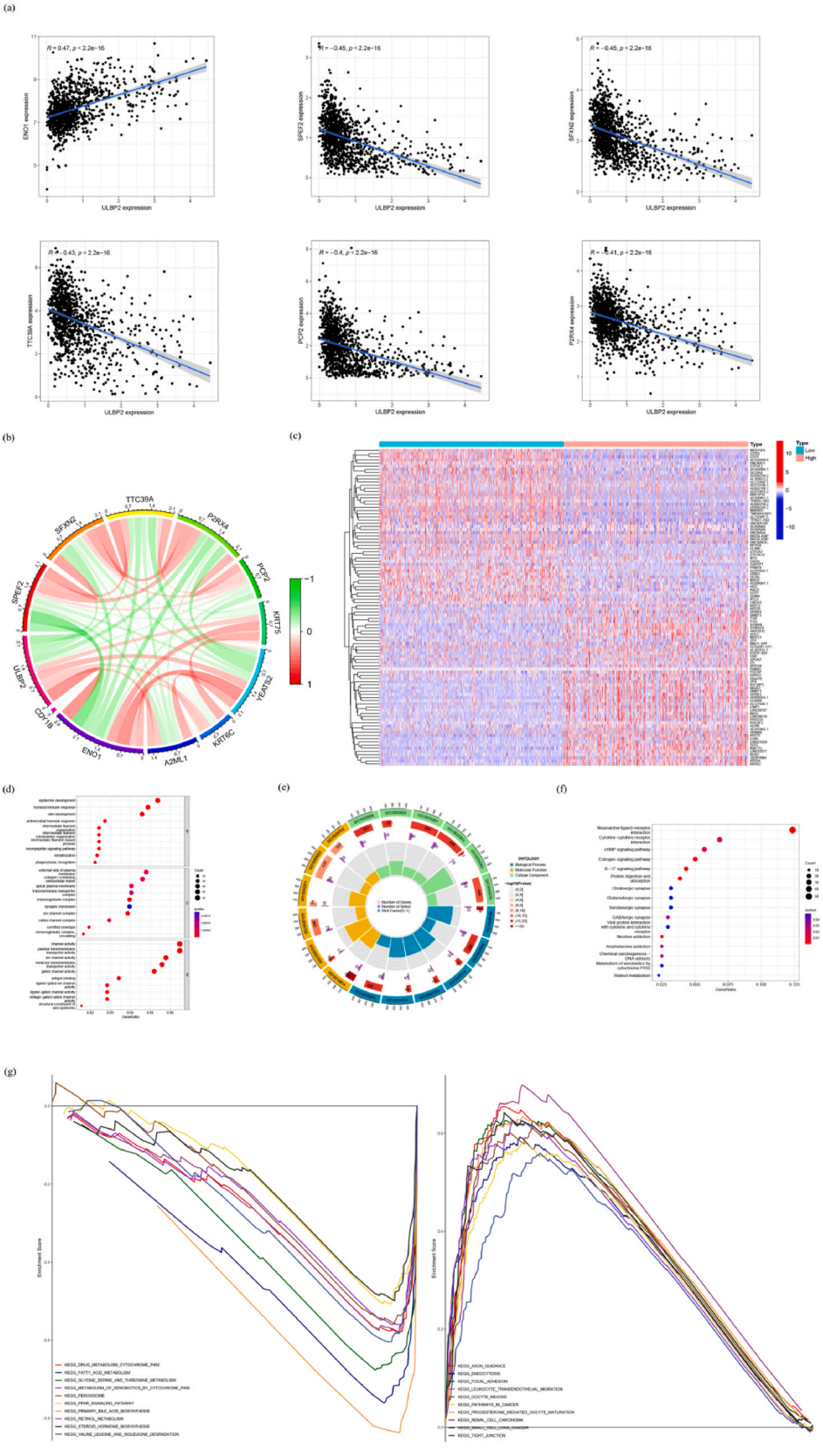

(caption on next page)

Fig. 5. Analysis of co-expressed genes of ULBP2. **(a)** the correlation of ENO1, SPEF2, SFXN2, TTC39A, PCP2 and P2RX4 with ULBP2. Statistical methods is pearson correlation analysis. **(b)** circle graph showed 5 genes with the smallest correlation coefficient and the 5 genes with the largest correlation coefficient. **(c)** 100 genes differentially expressed in different expression groups of ULBP2. **(d–f)** GO and KEGG enrichment analyses of co-expressed genes of ULBP2. **(g)** Gene sets enriched in ULBP2 high and low expression group. NOM $p < 0.05$, and $|NES| > 1$ are the significance threshold.

a novel predictor of immune checkpoint inhibitors. Then, analysis of transcriptome and clinical data of BC patients revealed that ULBP2 expression was significantly associated with the clinical characters (age, gender and T stage) and poor prognosis of BC patients. GO and KEGG analysis were used in co-expressed genes of ULBP2, which demonstrated they were enriched in functions of epidermis development, humoral immune response and skin development predominantly and pathways of Neuroactive ligand−receptor interaction, Cytokine−cytokine receptor interaction and cAMP signaling. It has been confirmed by research that Tumor-infiltrating B-cells make ongoing humoral immune responses to exert valid anti-tumor immunity in BC [27]. In another study, inhibiting cAMP signaling can promote the migration of breast cancer cell [28]. The co-expressed genes of ULBP2 are related to them, indicating that ULBP2 may affect the progress of BC through humoral immune responses and cAMP signaling. GSEA analysis showed that ULBP2 high expression group was associated with focal adhesion, leukocyte transendothelial migration and endocytosis. In ULBP2 low expression group, the gene sets enriched in metabolic pathways, such as primary bile acid biosynthesis, fatty acid metabolism and glycine serine and threonine metabolism. Increasing evidences also show that BC is closely related to the biological function of fatty acid metabolism [29–32].

In summary, our study reveals that the IRGs model can effectively predict BC patients' prognosis. In addition, ULBP2 can also be a potential therapeutic target. Due to the lack of *vivo* and *vitro* experiments, further experimental studies are necessary to verify and improve the results of this study, we also need more data to improve the accuracy and performance of the model and further analysis about ULBP2 to expose more potential effects in BC.

Data availability statement

The data associated with our study has been not deposited into a publicly available repository. Because the data to support the findings of this study are available on reasonable request from the corresponding author.

CRediT authorship contribution statement

Guosheng Ren: Conceived and designed the experiments. **Yuxian Wei:** Conceived and designed the experiments. **Rui Feng:** Conceived and designed the experiments. **Rui Feng:** Performed the experiments; Analyzed and interpreted the data. **Jiali Xu:** Performed the experiments; Analyzed and interpreted the data; Wrote the paper. **Jiazhou Liu:** Contributed reagents, materials, Formal analysis; Performed the experiments. **Hongzhong Li:** Contributed reagents, materials, Formal analysis; Performed the experiments. **Jing Huang:** Contributed reagents, materials, Formal analysis; Performed the experiments. **Xiaoyu Wang:** Contributed reagents, materials, Formal analysis; Performed the experiments. **Chong Zhang:** Performed the experiments; Analyzed and interpreted the data. **Jing Wang:** Performed the experiments; Analyzed and interpreted the data.

Declaration of competing interest

The authors declare that they have no known competing financial interests or personal relationships that could have appeared to influence the work reported in this paper.

Acknowledgments

Thanks to the TCGA for providing the original data. And This work was supported by the National Natural Science Foundation of China [grant numbers No. 82173166, 81472475 and 81902343]; Natural Science Foundation of Chongqing [grant numbers cstc2021jcyj-msxmX0015]; and CQMU Program for Youth Innovation in Future Medicine [grant numbers NO.W0094].

References

[1] Y. Xu, J. Deng, L. Wang, et al., Identification of candidate genes associated with breast cancer prognosis, DNA Cell Biol. 39 (2020) 1205–1227.
[2] I. Mayer, V. Abramson, B. Lehmann, et al., New strategies for triple-negative breast cancer–deciphering the heterogeneity, Clin. Cancer Res. : an official journal of the American Association for Cancer Research 20 (2014) 782–790.
[3] Q. Zhu, G. Wang, Y. Guo, et al., LncRNA H19 is a major mediator of doxorubicin chemoresistance in breast cancer cells through a cullin4A-MDR1 pathway, Oncotarget 8 (2017) 91990–92003.
[4] B. Li, E. Severson, J. Pignon, et al., Comprehensive analyses of tumor immunity: implications for cancer immunotherapy, Genome Biol. 17 (2016) 174.
[5] F. Varn, D. Mullins, H. Arias-Pulido, et al., Adaptive immunity programmes in breast cancer, Immunology 150 (2017) 25–34.
[6] R. Vonderheide, S. Domchek, A. Clark, Immunotherapy for breast cancer: what are we missing? Clin. Cancer Res. : an official journal of the American Association for Cancer Research 23 (2017) 2640–2646.
[7] S. Woo, L. Corrales, T. Gajewski, Innate immune recognition of cancer, Annu. Rev. Immunol. 33 (2015) 445–474.
[8] E.M. de Kruijf, A. Sajet, J.G. van Nes, et al., NKG2D ligand tumor expression and association with clinical outcome in early breast cancer patients: an observational study, BMC Cancer 12 (2012) 24.

[9] J. Fu, H. Sun, F. Xu, et al., RUNX regulated immune-associated genes predicts prognosis in breast cancer, Front. Genet. 13 (2022), 960489.
[10] R. Zheng, C. Wan, S. Mei, et al., Cistrome Data Browser: expanded datasets and new tools for gene regulatory analysis, Nucleic Acids Res. 47 (2019) D729–D735.
[11] D. Otasek, J. Morris, J. Bouças, et al., Cytoscape Automation: empowering workflow-based network analysis, Genome Biol. 20 (2019) 185.
[12] N. Nagarsheth, M. Wicha, W. Zou, Chemokines in the cancer microenvironment and their relevance in cancer immunotherapy, Nat. Rev. Immunol. 17 (2017) 559–572.
[13] R. Bremnes, K. Al-Shibli, T. Donnem, et al., The role of tumor-infiltrating immune cells and chronic inflammation at the tumor site on cancer development, progression, and prognosis: emphasis on non-small cell lung cancer, J. Thorac. Oncol. : official publication of the International Association for the Study of Lung Cancer 6 (2011) 824–833.
[14] T. Li, J. Fan, B. Wang, et al., TIMER: a web server for comprehensive analysis of tumor-infiltrating immune cells, Cancer Res. 77 (2017) e108–e110.
[15] Taiwen Li, Jingxin Fu, Zexian Zeng, et al., TIMER2.0 for analysis of tumor-infiltrating immune cells, Nucleic Acids Res. (2020) W509–W514.
[16] F. Gajewski Thomas, Schreiber Hans, Yang-Xin Fu, Innate and adaptive immune cells in the tumor microenvironment, Nat. Immunol. 14 (10) (2013) 1014–1022.
[17] O. Li Ming, Natalie Wolf, H. Raulet David, et al., Innate immune cells in the tumor microenvironment, Cancer Cell 39 (6) (2021) 725–729.
[18] H. Liang, Y. Li, MiR-873, as a suppressor in cervical cancer, inhibits cells proliferation, invasion and migration via negatively regulating ULBP2, Genes & genomics 42 (2020) 371–382.
[19] T. Kegasawa, T. Tatsumi, T. Yoshioka, et al., Soluble UL16-binding protein 2 is associated with a poor prognosis in pancreatic cancer patients, Biochem. Biophys. Res. Commun. 517 (2019) 84–88.
[20] E. Karamitopoulou, The tumor microenvironment of pancreatic cancer, Cancers 12 (10) (2020) 3076.
[21] N.M. Anderson, M.C. Simon, The tumor microenvironment, Curr. Biol. 30 (16) (2020) R921. –R5.
[22] S. Sui, X. An, C. Xu, et al., An immune cell infiltration-based immune score model predicts prognosis and chemotherapy effects in breast cancer, Theranostics 10 (26) (2020) 11938–11949.
[23] Y. Grabovska, A. Mackay, P. O'Hare, et al., Pediatric pan-central nervous system tumor analysis of immune-cell infiltration identifies correlates of antitumor immunity, Nat. Commun. 11 (1) (2020) 4324.
[24] D.A. Braun, Y. Hou, Z. Bakouny, et al., Interplay of somatic alterations and immune infiltration modulates response to PD-1 blockade in advanced clear cell renal cell carcinoma, Nat Med 26 (6) (2020) 909–918.
[25] S. Vranic, F.S. Cyprian, Z. Gatalica, et al., PD-L1 status in breast cancer: current view and perspectives, Semin. Cancer Biol. 72 (2021) 146–154.
[26] L. Liu, X. Bai, J. Wang, et al., Combination of TMB and CNA stratifies prognostic and predictive responses to immunotherapy across metastatic cancer, Clin. Cancer Res. 25 (24) (2019) 7413–7423.
[27] S. Garaud, L. Buisseret, C. Solinas, et al., Tumor infiltrating B-cells signal functional humoral immune responses in breast cancer, JCI Insight 5 (18) (2019), e129641.
[28] H. Dong, K.P. Claffey, S. Brocke, et al., Inhibition of breast cancer cell migration by activation of cAMP signaling, Breast Cancer Res. Treat. 152 (1) (2015) 17–28.
[29] Y. Tang, W. Tian, J. Xie, et al., Prognosis and dissection of immunosuppressive microenvironment in breast cancer based on fatty acid metabolism-related signature, Front. Immunol. 13 (2022), 843515.
[30] C.J. Fabian, B.F. Kimler, S.D. Hursting, Omega-3 fatty acids for breast cancer prevention and survivorship, Breast Cancer Res. 17 (1) (2015) 62.
[31] G.B. Ferraro, A. Ali, A. Luengo, et al., Fatty ACID synthesIS IS required for breast cancer brain metastasIS, Nat Cancer 2 (4) (2021) 414–428.
[32] P.B. Yang, P.P. Hou, F.Y. Liu, et al., Blocking PPARγ interaction facilitates Nur 77 interdiction of fatty acid uptake and suppresses breast cancer progression, Proc Natl Acad Sci U S A 117 (44) (2020) 27412–27422.